

Low-dimensional antiferromagnetic fluctuations in the heavy-fermion paramagnetic ladder compound UTe_2

W. Knafo¹, G. Knebel², P. Steffens³, K. Kaneko^{4,5}, A. Rosuel², J.-P. Brison², J. Flouquet², D. Aoki⁶, G. Lapertot² and S. Raymond⁷

¹Laboratoire National des Champs Magnétiques Intenses-EMFL, CNRS,

Université Grenoble Alpes, INSA-T, Université Toulouse 3, 31400 Toulouse, France

²Université Grenoble Alpes, CEA, Grenoble INP, IRIG, PHELIQS, 38000 Grenoble, France


³Institut Laue Langevin, 71 av des Martyrs, CS 20156, 38042 Grenoble, France

⁴Materials Sciences Research Center, Japan Atomic Energy Agency, Tokai, Ibaraki 319-1195, Japan

⁵Advanced Science Research Center, Japan Atomic Energy Agency, Tokai, Ibaraki 319-1195, Japan

⁶Institute for Materials Research, Tohoku University, Ibaraki 311-1313, Japan

⁷Université Grenoble Alpes, CEA, IRIG, MEM, MDN, 38000 Grenoble, France

 (Received 24 June 2021; revised 24 August 2021; accepted 25 August 2021; published 14 September 2021)

Inelastic-neutron-scattering measurements were performed on a single crystal of the heavy-fermion paramagnet UTe_2 above its superconducting temperature. We confirm the presence of antiferromagnetic fluctuations with the incommensurate wave-vector $\mathbf{k}_1 = (0, 0.57, 0)$. A quasielastic signal is found, whose momentum-transfer dependence is compatible with fluctuations of magnetic moments $\mu \parallel \mathbf{a}$ with a sine-wave modulation of wave-vector \mathbf{k}_1 and in-phase moments on the nearest U atoms. Low dimensionality of the magnetic fluctuations, consequence of the ladder structure, is indicated by weak correlations along the direction \mathbf{c} . These fluctuations saturate below the temperature $T_1^* \simeq 15$ K, in possible relation with anomalies observed in thermodynamic, electrical-transport, and nuclear-magnetic-resonance measurements. The absence or weakness of ferromagnetic fluctuations in our data collected at temperatures down to 2.1 K and energy transfers from 0.6 to 7.5 meV is emphasized. These results constitute constraints for models of magnetically mediated superconductivity in UTe_2 .

DOI: [10.1103/PhysRevB.104.L100409](https://doi.org/10.1103/PhysRevB.104.L100409)

The discovery of superconductivity at temperatures below $T_{sc} \simeq 1.6$ K in the heavy-fermion paramagnet UTe_2 [1,2] opened a breach in correlated-electron physics. UTe_2 was presented as a candidate for topological superconductivity, whose triplet and chiral characters have been proposed [1–11]. It turned rapidly out that this system is a unique model to study the electronic correlations and their feedback on magnetism and superconductivity [12–16]. A competition between different superconducting pairing mechanisms was indicated from the observation of multiple superconducting phases stabilized near quantum magnetic instabilities under pressure and magnetic field [17–27]. UTe_2 was first suspected to be a nearly ferromagnet in which ferromagnetic fluctuations were thought to lead to triplet superconductivity [13]. Longitudinal magnetic fluctuations were evidenced by NMR [28] and muon-spin relaxation measurements [29], but these studies could not unambiguously distinguish ferromagnetic and antiferromagnetic fluctuations. The nature of magnetic order induced under pressure [17] also constitutes an open question: Ferromagnetism was first suggested [23,24], but antiferromagnetism was proposed from more recent studies [22,27,30,31]. In addition, UTe_2 crystallizes in an *Immm* orthorhombic structure, where the U atoms form a two-leg ladder structure with legs along \mathbf{a} and rungs along \mathbf{c} [see Figs. 1(a) and 1(b)] [15,26,32]. Therefore, one could suspect

that low dimensionality may impact superconducting pairing too.

Inelastic neutron scattering is wave-vector-resolved and allows directly determining whether magnetic fluctuations are ferromagnetic or antiferromagnetic. A first neutron-scattering study of UTe_2 by time-of-flight spectroscopy on an assembly of 61 crystals offering a total mass of 700 mg and mosaicity of $\simeq 15^\circ$ led to the identification of antiferromagnetic fluctuations with the incommensurate wave-vectors $\mathbf{k}_1 = (0, 0.57, 0)$ and $\mathbf{k}_2 = (0, 0.43, 0)$ [expressed in reciprocal lattice units (rlu) and defined within the first Brillouin zone] [33]. Here, we present a neutron-scattering study using the triple-axis spectrometer Thales at the Institut Laue Langevin in Grenoble. A large single crystal of UTe_2 with a mass of 241 mg and a mosaicity of $\lesssim 2^\circ$ allowed a fine experimental resolution (see the Supplemental Material [34]). We confirm the presence of magnetic fluctuations with wave-vector \mathbf{k}_1 and do not see clear signatures of ferromagnetic fluctuations with wave-vector $\mathbf{k} = 0$. A low-dimensional character related with the ladder structure of the U atoms is emphasized, and the temperature evolution of the antiferromagnetic fluctuations with wave-vector \mathbf{k}_1 is carefully investigated.

Figure 2 presents energy scans measured at different momentum transfers \mathbf{Q} and $T = 2.1$ K for energy transfers $0.6 \leq E \leq 7.5$ meV. A large signal at the momentum transfer

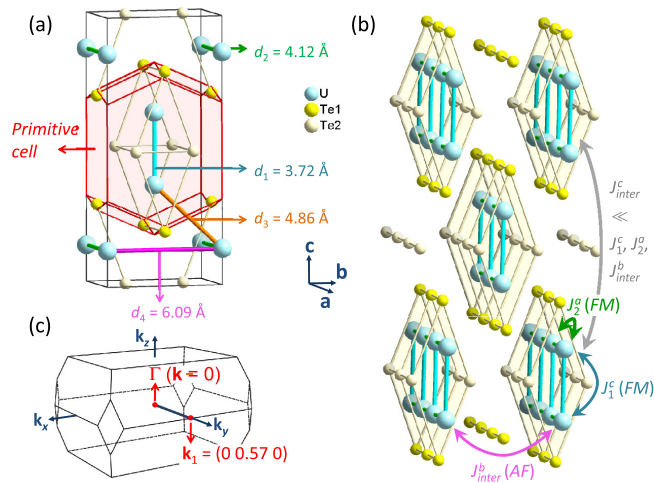


FIG. 1. (a) Orthorhombic cell and Wigner-Seitz primitive cell, and identification of the four shortest distances (from neutron diffraction at $T = 2.7$ K [32]), (b) extended structure emphasizing the ladder structure of U atoms, and (c) Brillouin zone of UTe_2 . A phenomenological magnetic-exchange scheme implied in the magnetic-fluctuations mode with wave-vector \mathbf{k}_1 is indicated in (b) (details are given in the text).

$\mathbf{Q}_1 = (0, 1.43, 0)$ indicates the presence of strong antiferromagnetic fluctuations at the incommensurate wave-vector $\mathbf{k}_1 = (0, 0.57, 0)$ [from $\mathbf{Q}_1 = \tau - \mathbf{k}_1$, where $\tau = (0, 2, 0)$ is a nuclear Bragg position]. \mathbf{k}_1 is close to the Brillouin-

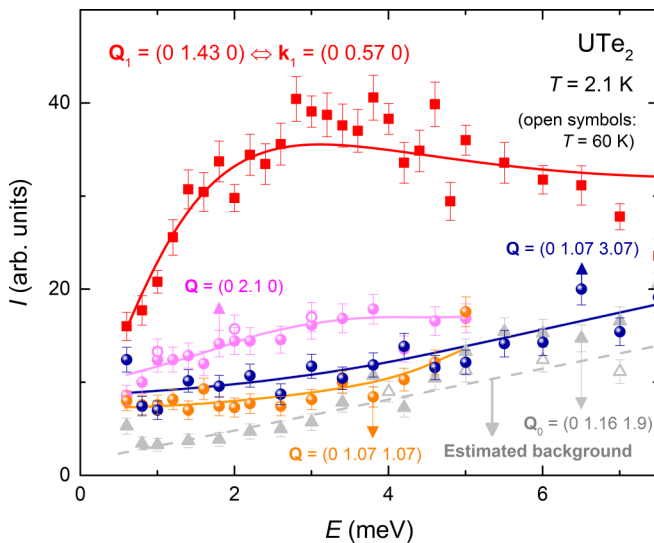


FIG. 2. Energy scans measured at the temperature $T = 2.1$ K and the momentum transfers $\mathbf{Q}_1 = (0, 1.43, 0)$ characteristic of antiferromagnetic fluctuations (red squares), $\mathbf{Q} = (0, 2.1, 0)$, $\mathbf{Q} = (0, 1.07, 1.07)$, and $\mathbf{Q} = (0, 1.07, 3.07)$ characteristic of ferromagnetic fluctuations (circles), and $\mathbf{Q}_0 = (0, 1.16, 1.9)$ characteristic of the background (gray triangles). A few points are shown at $T = 60$ K and the momentum transfers $\mathbf{Q} = (0, 2.1, 0)$ and $\mathbf{Q} = (0, 1.16, 1.9)$ (open symbols). Lines correspond to a fit to the data by a quasielastic Lorentzian shape at the momentum transfer \mathbf{Q}_1 to a fit to the data by a linear shape at the momentum transfer $\mathbf{Q} = (0, 1.16, 1.9)$ and to guides to the eyes at the other momentum transfers.

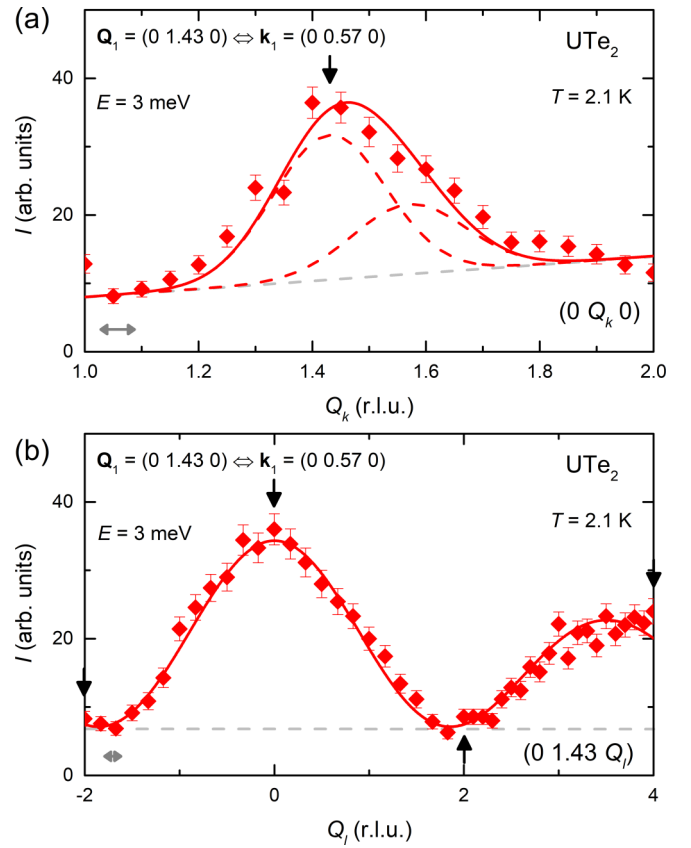


FIG. 3. (a) $(0, Q_k, 0)$ and (b) $(0, 1.43, Q_l)$ scans at the energy transfer $E = 3$ meV and the temperature $T = 2.1$ K. Gray dashed lines correspond to the estimated background. Gray double arrows in panels (a) and (b) indicate the full width at half maximum of Q_k and Q_l elastic scans around the Bragg peaks at positions $(0, 2, 0)$ and $(0, 0, 4)$, respectively. Red lines correspond to fit to the data as described in the Supplemental Material [34].

zone boundary [see Fig. 1(c)]. The momentum transfer $\mathbf{Q} = (0, 1.16, 1.9)$, chosen far from \mathbf{Q}_1 (and with the same modulus), is characteristic of a background without magnetic fluctuations. A few points collected at $T = 60$ K indicate a nearly temperature-independent background. Spectra at three momentum transfers $\mathbf{Q} = (0, 2.1, 0)$, $(0, 1.07, 1.07)$, and $(0, 1.07, 3.07)$, expected to characterize ferromagnetic fluctuations with wave-vector $\mathbf{k} \simeq 0$, present intensities near to the background level [35]. At $\mathbf{Q} = (0, 2.1, 0)$, the intensity is slightly higher than at the two other ferromagnetic positions, but similar intensities measured at $T = 2.1$ and 60 K indicate a presumably nonmagnetic signal. Within the experimental window investigated here ($T \geq 2.1$ K and $0.6 \leq E \leq 7.5$ meV), we do not identify, thus, any clear signature of ferromagnetic fluctuations in UTe_2 .

\mathbf{Q} dependences of the antiferromagnetic signal centered at \mathbf{Q}_1 , measured at the energy transfer $E = 3$ meV and at the temperature $T = 2.1$ K, are presented in Fig. 3. The $(0, Q_k, 0)$ scan shown in Fig. 3(a) indicates an asymmetric anomaly of maximal intensity near $\mathbf{Q}_1 = (0, 1.43, 0)$ with a shoulder for $Q_k > 1.43$. It can be fitted by two Gaussian contributions of same full width at half maximum $\kappa = 0.24$ rlu, corresponding to a correlation length $\xi_b \simeq 4b$, where $b = 6.09$ Å [32], along

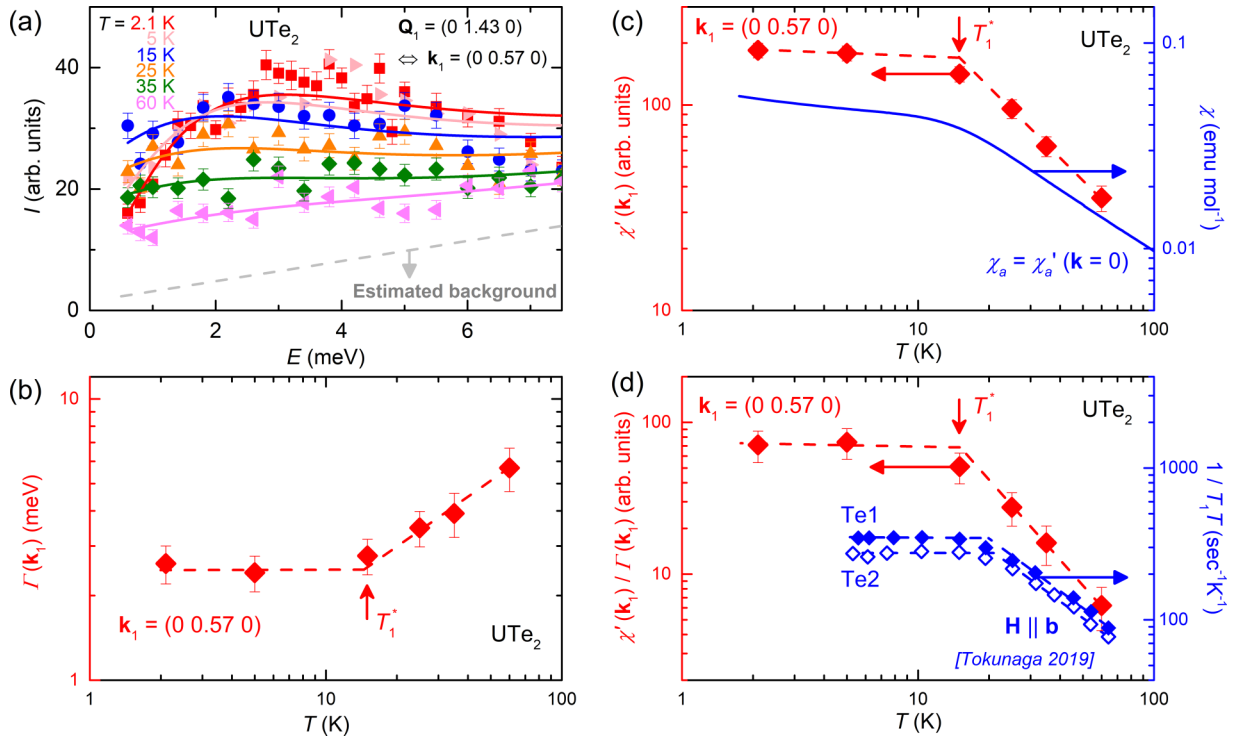


FIG. 4. (a) Energy scans measured at $\mathbf{Q}_1 = (0, 1.43, 0)$ and temperatures T from 2.1 to 60 K. Full lines are fits to the data assuming a Lorentzian shape, and the dashed line indicates the estimated background. Temperature dependence, on log-log scales, (b) of the relaxation rate $\Gamma(\mathbf{k}_1)$, (c) of the real part of the static susceptibility $\chi'(\mathbf{k}_1)$ and the bulk magnetic susceptibility $\chi_a = M/H$ measured in a magnetic-field $\mu_0\mathbf{H} \parallel \mathbf{a}$ of 0.1 T, and (d) of the ratio $\chi'(\mathbf{k}_1)/\Gamma(\mathbf{k}_1)$ and of the NMR relaxation rate $1/T_1T$ measured on the Te1 and Te2 sites in a magnetic-field $\mathbf{H} \parallel \mathbf{b}$ (from Ref. [28]). In panels (c) and (d), left and right log scales have the same number of decades to allow direct comparison between plotted data, and the two scales were adjusted together so that the two sets of data merge at high temperatures.

the direction \mathbf{b} . The contribution centered at the momentum transfer $\mathbf{Q}_1 = (0, 1.43, 0)$, corresponding to the wave-vector $\mathbf{k}_1 = (0, 0.57, 0)$, is twice more intense than that centered at the momentum transfer $\mathbf{Q}_2 = (0, 1.58, 0)$, corresponding to the wave-vector $\mathbf{k}_2 = (0, 0.42, 0)$. In the following, focus will be given to the dominant magnetic-fluctuations mode at wave-vector \mathbf{k}_1 . $(0, Q_k, 0)$ scans at different energy transfers E , shown in the Supplemental Material [34], further indicate that the magnetic fluctuations signal at the wave-vector $\mathbf{k}_1 = (0, 0.57, 0)$ is weakly or not dispersive. In Fig. 3(b), a $(0, 1.43, Q_l)$ scan presents a damped sine-wave evolution of the scattered intensity. Best fit to the data is performed assuming (i) fluctuating magnetic moments $\mu \parallel \mathbf{a}$ and (ii) in-phase magnetic moments on the two U's of the primitive cell (see Fig. 1(a) and the Supplemental Material [34]). The sine-wave modulation indicates that, within first approximation, the correlations along \mathbf{c} can be neglected, i.e., that the inter-ladder magnetic coupling along \mathbf{c} is weak. A first component $k_{1,h} = 0$ of the propagation vector \mathbf{k}_1 is implicitly assumed here and in Ref. [33]. Indeed, strong correlations along the ladder direction \mathbf{a} are expected from the short-distance $d_2 = 4.12 \text{ \AA}$ between U atoms along \mathbf{a} . For these reasons, one can safely expect that the fluctuations with wave-vector \mathbf{k}_1 imply correlations with in-phase fluctuating moments along \mathbf{a} . We can further conclude that the antiferromagnetic fluctuations investigated here are low dimensional and that they are char-

acterized by a set of equivalent or nearly equivalent lines of wave-vectors $\mathbf{k}_L = (0, 0.43, \delta)$ and $(0, 0.57, \delta)$, which include \mathbf{k}_1 and \mathbf{k}_2 (see the Supplemental Material [34]).

Figure 4(a) shows spectra measured at the momentum transfer $\mathbf{Q}_1 = (0, 1.43, 0)$ for a large set of temperatures T from 2.1 to 60 K. The increase in T leads to a progressive decrease and broadening of the antiferromagnetic signal. We fitted data shown in Fig. 4(a) assuming a quasielastic Lorentzian variation of the imaginary part of the dynamical susceptibility $\chi''(\mathbf{Q}_1, E)$ (see the Supplemental Material [34]). The temperature variations of the relaxation rate $\Gamma(\mathbf{k}_1)$ and of the real part of the static susceptibility $\chi'(\mathbf{k}_1)$ extracted from these fits are plotted within log-log scales in Figs. 4(b) and 4(c). When the temperature is lowered, the strengthening of antiferromagnetic fluctuations is evidenced by the decrease in $\Gamma(\mathbf{k}_1)$ and the increase in $\chi'(\mathbf{k}_1)$, which both saturate at temperatures below $T_1^* \simeq 15 \text{ K}$. T_1^* and the low-temperature value $\Gamma(\mathbf{k}_1) \simeq 2.5 \text{ meV} \simeq 2k_B T_1^*$ are characteristic of the antiferromagnetic fluctuations with wave-vector \mathbf{k}_1 .

Anomalies are observed at temperatures near T_1^* in various physical properties. The bulk magnetic susceptibility $\chi_a = M/H$, where M is the magnetization and $\mu_0 H = 0.1 \text{ T}$, a magnetic field applied along the easy magnetic axis \mathbf{a} , is compared to $\chi'(\mathbf{k}_1)$ in Fig. 4(c). Knowing that $\chi_a = \chi'_a(\mathbf{k} = 0)$ and $\chi'(\mathbf{k}_1) = \chi'_a(\mathbf{k}_1)$ (since the magnetic fluctuations with

wave-vector \mathbf{k}_1 were attributed to magnetic moments $\mu \parallel \mathbf{a}$, both quantities are expected to converge at temperatures at which intersite magnetic correlations have vanished, i.e., presumably $T \gtrsim 100$ K. A broad kink in χ_a is observed at the temperature $T_{\chi_a}^{\text{kink}} \simeq 15$ K $\simeq T_1^*$. Maxima in the electronic heat capacity [36] and electrical resistivity measured with a current $\mathbf{I} \parallel \mathbf{c}$ [37] and minima in the thermal expansion measured with lengths $\mathbf{L} \parallel \mathbf{b}, \mathbf{c}$ [36,38], and thermoelectric power measured with a current $\mathbf{I} \parallel \mathbf{a}$ [39] were also observed at a temperature of $\simeq 15$ K. These anomalies may result from the development of antiferromagnetic fluctuations with wave-vector \mathbf{k}_1 and their possible feedbacks on the Fermi surface. Figure 4(d) presents a comparison of $\chi'(\mathbf{k}_1)/\Gamma(\mathbf{k}_1)$ extracted here and the NMR relaxation rate $1/T_1T$, measured in a magnetic field $\mathbf{H} \parallel \mathbf{b}$ by Tokunaga *et al.* (for the two sites Te1 and Te2) [28]. These two quantities are dominated by fluctuations of magnetic moments $\mu \parallel \mathbf{a}$ and vary similarly, increasing with decreasing temperatures before saturating at low temperature. $1/T_1T$ saturates below a temperature of $\simeq 15$ K near T_1^* . Knowing that $1/T_1T$ consists of a sum of $\chi'(\mathbf{k})/\Gamma(\mathbf{k})$ over the reciprocal space (see Supplemental Material [34]), the magnetic fluctuations at \mathbf{k}_1 (and its equivalent positions \mathbf{k}_L) may contribute significantly to $1/T_1T$. The slower T variation of $1/T_1T$, in comparison with that of $\chi'(\mathbf{k}_1)/\Gamma(\mathbf{k}_1)$ may be due to the contribution of fluctuations at wave vectors far from \mathbf{k}_1 . The question of low-energy ferromagnetic fluctuations (not observed here) and, thus, of their possible contribution to $1/T_1T$, which is sensitive to energies $E \rightarrow 0$, remains open.

A similar relationship between anomalies in bulk properties and magnetic fluctuations was observed in other heavy-fermion paramagnets [40]. In the prototypical heavy-fermion paramagnet CeRu₂Si₂, the characteristic temperature $T_1^* \simeq 10$ K of longitudinal antiferromagnetic fluctuations [41] is comparable to those of anomalies in the magnetic susceptibility [42], thermal expansion [43], and NMR relaxation rate [44]. The situation in UTe₂ is more complex. In addition to the temperature scale of $\simeq 15$ K considered earlier, a second temperature scale of $\simeq 35$ K can be identified from maxima in the magnetic susceptibility χ_b measured with $\mathbf{H} \parallel \mathbf{b}$ (hard magnetic axis) [45] in the Hall coefficient [39] and electrical resistivity [18] measured with a current $\mathbf{I} \parallel \mathbf{a}$. Further experiments are needed to determine the relationship between the 15-K and 35-K anomalies and to test if a second and higher-energy magnetic-fluctuations mode could be present.

The possible coexistence of ferromagnetic and antiferromagnetic couplings in the ladder structure of UTe₂ was theoretically discussed in Ref. [15], and a first report of antiferromagnetic fluctuations was performed in Ref. [33]. Thanks to a careful investigation of this antiferromagnetic-fluctuations mode, we emphasize here its quasielastic and low-dimensional characteristics. It can be visualized as fluctuations of magnetic moments $\mu \parallel \mathbf{a}$ with the following phenomenological scheme: (i) an interladder antiferromagnetic coupling J_{inter}^b (AF) along \mathbf{b} ending in sine-wave modulation with wave-vector \mathbf{k}_1 of the moments, (ii) intraladder ferromagnetic couplings J_1^c (FM) along \mathbf{c} and J_2^a (FM) along \mathbf{a} , and (iii) a weak interladder magnetic coupling J_{inter}^c along \mathbf{c} [see Fig. 1(a)] [46]. As shown in Fig. 1(a), the two

nearest-neighbor interactions correspond to the intraladder exchanges J_1^c and J_2^a (U-U distances $d_1 = 3.72$ and $d_2 = 4.12$ Å, respectively). The third shortest U-U distance $d_3 = 4.86$ Å is along a tilted direction with components along the three crystallographic axes \mathbf{a} , \mathbf{b} , and \mathbf{c} . Since the fourth shortest distance $d_4 = 6.09$ Å, along direction \mathbf{b} , is much bigger than the three previous ones, the magnetic exchange J_{inter}^b leading to a modulation along \mathbf{b} may result from a subtle combination of exchange paths, possibly implying electronic processes along the tilted direction. A theory describing microscopically the magnetic exchange interactions may help understanding how low dimensionality affects the magnetic fluctuations and how it is related to the large-energy scale $\Gamma(\mathbf{k}_1) \simeq 2.5$ meV reported here.

\mathbf{Q} modulations of a magnetic-fluctuations signal similar to those reported here for UTe₂ were observed by inelastic neutron scattering in other low-dimensional magnets whose primitive cell contains several magnetic ions as the magnetic ladder Sr₁₄Cu₂₄O₄₁ [47,48], the layered paramagnet Sr₃Ru₂O₇ [49], the antiferromagnet YBa₂Cu₃O_{6.2} [50], and superconductors YBa₂Cu₃O_{6.85} [51] and CaKFe₄As₄ [52]. It has been argued that a more robust superconducting pairing is expected for two-dimensional rather than three-dimensional itinerant magnets [53]. A low-dimensional character of the magnetic fluctuations may, thus, be of importance for the development of superconductivity in UTe₂. The question of the role of ferromagnetic fluctuations for the development of a superconducting phase, often suspected to be triplet, needs to be clarified. Ferromagnetic fluctuations were not observed here, within the investigated experimental window $0.6 \leq E \leq 7.5$ meV at $T = 2.1$ K, but Duan *et al.* reported a small signal at the ferromagnetic momentum transfer $\mathbf{Q} = (0, 1, 1)$ at $E \simeq 0.4$ meV and $T = 300$ mK [33]. Unambiguous experimental evidence for ferromagnetic fluctuations is now needed. We note that, in the paramagnet Sr₂RuO₄, a former candidate for triplet superconductivity, intense incommensurate antiferromagnetic fluctuations were found to coexist with weak and broad in \mathbf{Q} space quasiferromagnetic fluctuations [54,55]. Conversely, triplet superconductivity was proposed to occur in UPT₃ where only antiferromagnetic fluctuations were observed [56,57]. Our finding that the antiferromagnetic fluctuations imply ferromagnetically coupled U atoms on the ladders may be of importance. Indeed, it is compatible with the proposition of pseudotriplet superconductivity induced by a ferromagnetic interaction between U atoms of the ladder rungs without necessarily implying ferromagnetic fluctuations [8,15,58]. In the future, challenges will be to determine precisely the respective roles of antiferromagnetic and ferromagnetic fluctuations and low dimensionality for the stabilization of different superconducting phases in UTe₂. The topology and possible low dimensionality of some Fermi-surface sheets, which set in at low temperatures, also play a role for superconductivity [8,14,15] and would merit further consideration too. We note that, during the publication process of this Letter, the opening of a gap in the magnetic-excitations spectrum with the wave-vector \mathbf{k}_1 was reported in the superconducting phase [59,60], confirming that the low-dimensional antiferromagnetic fluctuations reported here play a role for superconductivity in UTe₂.

We acknowledge useful discussions with Y. Tokunaga, K. Ishida, and C. Simon. This work was supported by the ANR FRESKO and was partly supported by JSPS KAKENHI

Grants No. JP19H00646, No. 19K03756, No. JP20H00130, No. 20H01864, No. JP20K20889, No. JP20KK0061, and No. 21H04987.

- [1] S. Ran, C. Eckberg, Q.-P. Ding, Y. Furukawa, T. Metz, S. R. Saha, I.-L. Liu, M. Zic, H. Kim, J. Paglione, and N. P. Butch, *Science* **365**, 684 (2019).
- [2] D. Aoki, A. Nakamura, F. Honda, D. Li, Y. Homma, Y. Shimizu, Y. J. Sato, G. Knebel, J.-P. Brison, A. Pourret, D. Braithwaite, G. Lapertot, Q. Niu, M. Vališka, H. Harima, and J. Flouquet, *J. Phys. Soc. Jpn.* **88**, 043702 (2019).
- [3] J. Ishizuka, S. Sumita, A. Daido, and Y. Yanase, *Phys. Rev. Lett.* **123**, 217001 (2019).
- [4] G. Nakamine, S. Kitagawa, K. Ishida, Y. Tokunaga, H. Sakai, S. Kambe, A. Nakamura, Y. Shimizu, Y. Homma, D. Li, F. Honda, and D. Aoki, *J. Phys. Soc. Jpn.* **88**, 113703 (2019).
- [5] T. Metz, S. Bae, S. Ran, I.-Lin Liu, Y. S. Eo, W. T. Fuhrman, D. F. Agterberg, S. M. Anlage, N. P. Butch, and J. Paglione, *Phys. Rev. B* **100**, 220504(R) (2019).
- [6] S. Kittaka, Y. Shimizu, T. Sakakibara, A. Nakamura, D. Li, Y. Homma, F. Honda, D. Aoki, and K. Machida, *Phys. Rev. Research* **2**, 032014(R) (2020).
- [7] L. Jiao, S. Howard, S. Ran, Z. Wang, J. O. Rodriguez, M. Sigrist, Z. Wang, N. P. Butch, and V. Madhavan, *Nature (London)* **579**, 523 (2020).
- [8] T. Shishidou, H. G. Suh, P. M. R. Brydon, M. Weinert, and D. F. Agterberg, *Phys. Rev. B* **103**, 104504 (2021).
- [9] I. M. Hayes, D. S. Wei, T. Metz, J. Zhang, Y. S. Eo, S. Ran, S. R. Saha, J. Collini, N. P. Butch, D. F. Agterberg, A. Kapitulnik, and J. Paglione, *Science* **373**, 797 (2021).
- [10] S. Bae, H. Kim, Y. S. Eo, S. Ran, I. lin Liu, W. T. Fuhrman, J. Paglione, N. P. Butch, and S. M. Anlage, *Nat. Commun.* **12**, 2644 (2021).
- [11] M. Sato and Y. Ando, *Rep. Prog. Phys.* **80**, 076501 (2017).
- [12] A. B. Shick, S.-i. Fujimori, and W. E. Pickett, *Phys. Rev. B* **103**, 125136 (2021).
- [13] J. Ishizuka and Y. Yanase, *Phys. Rev. B* **103**, 094504 (2021).
- [14] L. Miao, S. Liu, Y. Xu, E. C. Kotta, C.-J. Kang, S. Ran, J. Paglione, G. Kotliar, N. P. Butch, J. D. Denlinger, and L. A. Wray, *Phys. Rev. Lett.* **124**, 076401 (2020).
- [15] Y. Xu, Y. Sheng, and Y.-f. Yang, *Phys. Rev. Lett.* **123**, 217002 (2019).
- [16] K. Machida, *J. Phys. Soc. Jpn.* **89**, 033702 (2020).
- [17] D. Braithwaite, M. Vališka, G. Knebel, G. Lapertot, J.-P. Brison, A. Pourret, M. E. Zhitomirsky, J. Flouquet, F. Honda, and D. Aoki, *Commun. Phys.* **2**, 147 (2019).
- [18] W. Knafo, M. Vališka, D. Braithwaite, G. Lapertot, G. Knebel, A. Pourret, J.-P. Brison, J. Flouquet, and D. Aoki, *J. Phys. Soc. Jpn.* **88**, 063705 (2019).
- [19] A. Miyake, Y. Shimizu, Y. J. Sato, D. Li, A. Nakamura, Y. Homma, F. Honda, J. Flouquet, M. Tokunaga, and D. Aoki, *J. Phys. Soc. Jpn.* **88**, 063706 (2019).
- [20] G. Knebel, W. Knafo, A. Pourret, Q. Niu, M. Vališka, D. Braithwaite, G. Lapertot, M. Nardone, A. Zitouni, S. Mishra, I. Sheikin, G. Seyfarth, J.-P. Brison, D. Aoki, and J. Flouquet, *J. Phys. Soc. Jpn.* **88**, 063707 (2019).
- [21] S. Ran, I.-L. Liu, Y. S. Eo, D. J. Campbell, P. Neves, W. T. Fuhrman, S. R. Saha, C. Eckberg, H. Kim, J. Paglione, D. Graf, J. Singleton, and N. P. Butch, *Nat. Phys.* **15**, 1250 (2019).
- [22] D. Aoki, F. Honda, G. Knebel, D. Braithwaite, A. Nakamura, D. Li, Y. Homma, Y. Shimizu, Y. J. Sato, J.-P. Brison, and J. Flouquet, *J. Phys. Soc. Jpn.* **89**, 053705 (2020).
- [23] S. Ran, H. Kim, I.-Lin Liu, S. R. Saha, I. Hayes, T. Metz, Y. S. Eo, J. Paglione, and N. P. Butch, *Phys. Rev. B* **101**, 140503(R) (2020).
- [24] W. C. Lin, D. J. Campbell, S. Ran, I.-L. Liu, H. Kim, A. H. Nevidomskyy, D. Graf, N. P. Butch, and J. Paglione, *npj Quantum Mater.* **5**, 68 (2020).
- [25] G. Knebel, M. Kimata, M. Vališka, F. Honda, D. Li, D. Braithwaite, G. Lapertot, W. Knafo, A. Pourret, Y. J. Sato, Y. Shimizu, T. Kihara, J.-P. Brison, J. Flouquet, and D. Aoki, *J. Phys. Soc. Jpn.* **89**, 053707 (2020).
- [26] W. Knafo, M. Nardone, M. Vališka, A. Zitouni, G. Lapertot, D. Aoki, G. Knebel, and D. Braithwaite, *Commun. Phys.* **4**, 40 (2021).
- [27] D. Aoki, M. Kimata, Y. J. Sato, G. Knebel, F. Honda, A. Nakamura, D. Li, Y. Homma, Y. Shimizu, W. Knafo, D. Braithwaite, M. Vališka, A. Pourret, J.-P. Brison, and J. Flouquet, *J. Phys. Soc. Jpn.* **90**, 074705 (2021).
- [28] Y. Tokunaga, H. Sakai, S. Kambe, T. Hattori, N. Higa, G. Nakamine, S. Kitagawa, K. Ishida, A. Nakamura, Y. Shimizu, Y. Homma, D. Li, F. Honda, and D. Aoki, *J. Phys. Soc. Jpn.* **88**, 073701 (2019).
- [29] S. Sundar, S. Gheidi, K. Akintola, A. M. Côté, S. R. Dunsiger, S. Ran, N. P. Butch, S. R. Saha, J. Paglione, and J. E. Sonier, *Phys. Rev. B* **100**, 140502(R) (2019).
- [30] S. M. Thomas, F. B. Santos, M. H. Christensen, T. Asaba, F. Ronning, J. D. Thompson, E. D. Bauer, R. M. Fernandes, G. Fabbris, and P. F. S. Rosa, *Sci. Adv.* **6**, 42 (2020).
- [31] D. Li, A. Nakamura, F. Honda, Y. J. Sato, Y. Homma, Y. Shimizu, J. Ishizuka, Y. Yanase, G. Knebel, J. Flouquet, and D. Aoki, *J. Phys. Soc. Jpn.* **90**, 073703 (2021).
- [32] V. Hutanu, H. Deng, S. Ran, W. T. Fuhrman, H. Thoma, and N. P. Butch, *Acta Crystallogr., Sect. B: Struct. Sci., Cryst. Eng. Mater.* **76**, 137 (2020).
- [33] C. Duan, K. Sasmal, M. B. Maple, A. Podlesnyak, J.-X. Zhu, Q. Si, and P. Dai, *Phys. Rev. Lett.* **125**, 237003 (2020).
- [34] See Supplemental Material at <http://link.aps.org/supplemental/10.1103/PhysRevB.104.L100409> for details.
- [35] The momentum transfers $\mathbf{Q} = (0, 2.1, 0)$, $(0, 1.07, 1.07)$, and $(0, 1.07, 3.07)$ were chosen near, but not exactly at, the nuclear Bragg positions $\tau = (0, 2, 0)$, $(0, 1, 1)$, and $(0, 1, 3)$ corresponding to magnetic wave-vector $\mathbf{k} = 0$ to avoid contamination by the nuclear Bragg peaks.
- [36] K. Willa, F. Hardy, D. Aoki, D. Li, P. Wiecki, G. Lapertot, and C. Meingast [arXiv:2107.02706](https://arxiv.org/abs/2107.02706).
- [37] Y. S. Eo, S. R. Saha, H. Kim, S. Ran, J. A. Horn, H. Hodovanets, J. Collini, W. T. Fuhrman, A. H. Nevidomskyy, N. P. Butch, M. S. Fuhrer, and J. Paglione, [arXiv:2101.03102](https://arxiv.org/abs/2101.03102).

- [38] S. M. Thomas, C. Stevens, F. B. Santos, S. S. Fender, E. D. Bauer, F. Ronning, J. D. Thompson, A. Huxley, and P. F. S. Rosa, [arXiv:2103.09194](#).
- [39] Q. Niu, G. Knebel, D. Braithwaite, D. Aoki, G. Lapertot, G. Seyfarth, J.-P. Brison, J. Flouquet, and A. Poursat, *Phys. Rev. Lett.* **124**, 086601 (2020).
- [40] D. Aoki, W. Knafo, and I. Sheikin, *C. R. Phys.* **14**, 53 (2013).
- [41] W. Knafo, S. Raymond, P. Lejay, and J. Flouquet, *Nat. Phys.* **5**, 753 (2009).
- [42] P. Haen, J. Flouquet, F. Lapierre, P. Lejay, and G. Remenyi, *J. Low Temp. Phys.* **67**, 391 (1987).
- [43] C. Paulsen, A. Lacerda, L. Puech, P. Haen, P. Lejay, J. L. Tholence, J. Flouquet, and A. de Visser, *J. Low Temp. Phys.* **81**, 317 (1990).
- [44] K. Ishida, Y. Kawasaki, Y. Kitaoka, K. Asayama, H. Nakamura, and J. Flouquet, *Phys. Rev. B* **57**, R11054 (1998).
- [45] S. Ikeda, H. Sakai, D. Aoki, Y. Homma, E. Yamamoto, A. Nakamura, Y. Shiokawa, Y. Haga, and Y. Onuki, *J. Phys. Soc. Jpn.* **75**, 116 (2006).
- [46] The phenomenological inter-ladder magnetic couplings J_{inter}^b and J_{inter}^c introduced here may result from two successive “diagonal” interladder exchanges [along the third shortest U-U distance d_3 , see Figs. 1(a) and 1(b)].
- [47] L. P. Regnault, A. H. Moudden, J. P. Boucher, E. Lorenzo, A. Hiess, A. Vietkin, and A. Revcolevschi, *Physica B* **259**, 1038 (1999).
- [48] C. Boullier, Ph.D. thesis, University of Grenoble, 2005.
- [49] L. Capogna, E. M. Forgan, S. M. Hayden, A. Wildes, J. A. Duffy, A. P. Mackenzie, R. S. Perry, S. Ikeda, Y. Maeno, and S. P. Brown, *Phys. Rev. B* **67**, 012504 (2003).
- [50] M. Sato, S. Shamoto, J. M. Tranquada, G. Shirane, and B. Keimer, *Phys. Rev. Lett.* **61**, 1317 (1988).
- [51] S. Pailhès, Y. Sidis, P. Bourges, V. Hinkov, A. Ivanov, C. Ulrich, L. P. Regnault, and B. Keimer, *Phys. Rev. Lett.* **93**, 167001 (2004).
- [52] T. Xie, Y. Wei, D. Gong, T. Fennell, U. Stuhr, R. Kajimoto, K. Ikeuchi, S. Li, J. Hu, and H. Luo, *Phys. Rev. Lett.* **120**, 267003 (2018).
- [53] P. Monthoux and G. G. Lonzarich, *Phys. Rev. B* **63**, 054529 (2001).
- [54] A. Pustogow, Y. Luo, A. Chronister, Y.-S. Su, D. A. Sokolov, F. Jerzembeck, A. P. Mackenzie, C. W. Hicks, N. Kikugawa, S. Raghu, E. D. Bauer, and S. E. Brown, *Nature (London)* **574**, 72 (2019).
- [55] P. Steffens, Y. Sidis, J. Kulda, Z. Q. Mao, Y. Maeno, I. I. Mazin, and M. Braden, *Phys. Rev. Lett.* **122**, 047004 (2019).
- [56] G. Aeppli, E. Bucher, C. Broholm, J. K. Kjems, J. Baumann, and J. Hufnagl, *Phys. Rev. Lett.* **60**, 615 (1988).
- [57] H. Tou, Y. Kitaoka, K. Ishida, K. Asayama, N. Kimura, Y. Onuki, E. Yamamoto, Y. Haga, and K. Maezawa, *Phys. Rev. Lett.* **80**, 3129 (1998).
- [58] P. W. Anderson, *Phys. Rev. B* **32**, 499 (1985).
- [59] C. Duan, R. E. Baumbach, A. Podlesnyak, Y. Deng, C. Moir, A. J. Breindel, M. B. Maple, and P. Dai, [arXiv:2106.14424](#).
- [60] S. Raymond, W. Knafo, G. Knebel, K. Kaneko, J.-P. Brison, J. Flouquet, D. Aoki, and G. Lapertot, [arXiv:2107.13914](#).